PROOF COPY 005303JBO

Journal of Biomedical Optics 8(3), 1–0 (July 2003)

Application of an *ex ovo* chicken chorioallantoic membrane model for two-photon excitation photodynamic therapy of age-related macular degeneration

Kimberley S. Samkoe
David T. Cramb
University of Calgary
Department of Chemistry
2500 University Drive NW
Calgary, AB, Canada T2N 1N4
E-mail: dcramb@ucalgary.ca

Abstract. Two-photon excitation photodynamic therapy (TPE-PDT) is being investigated as a clinical treatment for age-related macular degeneration (AMD). TPE-PDT has the potential to provide a more specific and therefore advantageous therapy regime than traditional one-photon excitation PDT. The highly vascularized 8 to 9-day-old chicken chorioallantoic membrane (CAM) is used to model the rapid growth of blood vessels in the wet form of AMD. Using an *ex ovo* model system for the CAM, ablation studies were successful in mimicking the leaky vessels found in AMD. In addition, the distribution and localization of liposomal Verteporfin were investigated in order to characterize the photosensitizing drug *in vivo*. Localization of the photosensitizer appears to be greatest on the upper vessel wall, which indicates a potentially strong treatment locale for TPE-PDT. © *2003 Society of Photo-Optical Instrumentation Engineers.* [DOI: 10.1117/1.1577117]

Keywords: chorioallantoic membrane; photodynamic therapy; two-photon excitation; age-related macular degeneration.

Paper MM-05 received Nov. 7, 2002; revised manuscript received Dec. 20, 2002; accepted for publication Dec. 23, 2002.

PROOF COPY 005303JBO

1 Introduction

Age-related macular degeneration (AMD) is a disease commonly found in developed countries in people over the age of 60.[1] There are two forms of the disease, dry and wet AMD.[2,3] Dry AMD involves the death of cone cells in the macular region of the eye, collection of drusen proximal to the Bruch's membrane, and disruption of the pigmentation of the retinal pigment epithelium (RPE). The wet form of this disease exhibits the same physical symptoms as the dry form, but also prominently displays outward growth of blood vessels from the choriocapillaris, through Bruch's membrane and the RPE into the subretinal spaces. The blood vessels that form from the process of angiogenesis are often leaky and exude fluid into the space below the photoreceptors, possibly directly causing an increase in cone death and a resultant loss in vision. Although the wet form is found in only 10% of patients with AMD, it is responsible for over 90% of the vision loss associated with this disease.[4]

Photodynamic therapy (PDT) has been approved in many countries for treatment of AMD. When undergoing treatment, a patient is systemically administered a therapeutic volume of the photosensitizing agent, Verteporfin [a benzoporphyrin derivative mono acid (ring A), BPD-MA], which localizes in areas of high cellular reproduction. The drug is then promoted to its first excited state by irradiation with laser light ($\sim$680 nm). In type II PDT, the excitation energy can then be transferred, via the sensitizer's triplet manifold, to naturally occurring triplet oxygen, promoting the production of singlet oxygen. Singlet oxygen has the ability to diffuse into the surrounding tissue, causing destruction of living cells. The method of cell death is believed to be apoptotic in nature, although necrosis is also possible via PDT.

Currently, this method of treatment is the best option for patients with wet AMD, but there is a limitation that can confound achieving the maximum therapeutic effect. In the government-approved one-photon excitation PDT (OPE-PDT), the photosensitizer is necessarily excited along the entire path of the laser beam. Therefore, damage to healthy retinal tissue may result from activation of both endogenous and exogenous photosensitizers in the surrounding healthy tissue.

Recently, several investigations into an alternative mode of PDT have been initiated.[5–8] By using two-photon excitation (TPE) in the near-infrared region (NIR, $\lambda = 950$ to 750 nm), some problems of traditional OPE-PDT can, in principle, be overcome. The probability of TPE occurring is greatest in the focal plane of a strongly focused laser beam, and excitation volumes as small as 0.5 μm^3 can be achieved.[9] This reduced excitation volume could allow the photosensitizing drug to be selectively activated within a confined space, such as a blood vessel arising in the wet form of AMD or an individual cell. The application of TPE-PDT will allow treatment deeper into diseased tissue because mammalian tissue has a spectral window between 800 and 1100 nm.[7] This reduces the amount of light scatter and absorption by both diseased and healthy tissue that is observed in OPE-PDT.

In order to test the validity of TPE-PDT in AMD treatment, a model system has to be created that can be utilized to mimic several factors found in wet AMD. First the model must have blood vessels that are relatively the same size as

1083-3668/2003/$15.00 © 2003 SPIE

PROOF COPY 005303JBO

PROOF COPY 005303JBO

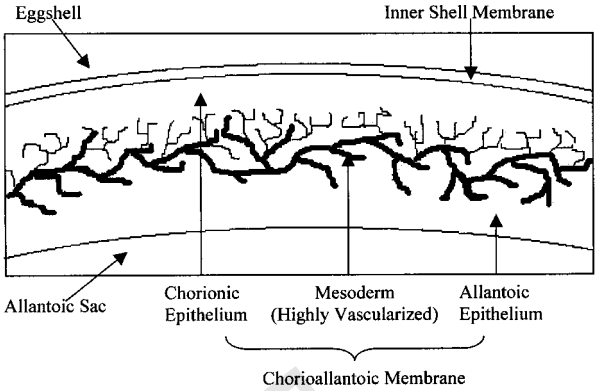

Fig. 1 An illustration of a cross-section of the chicken CAM. The highly vascularized mesoderm lies between the chorionic (proximal to the shell) and allantoic (distal to the shell) epitheliums.

those found in the human eye during wet AMD. Second, the blood vessels must be undergoing rapid angiogenesis. Third, the vessels preferably should be found in a relatively clear tissue that resembles the transparent retinal tissue. Finally, it should be possible to induce leaks in these vessels. The chorioallantoic membrane (CAM) of the chicken embryo meets all of these criteria. The CAM is also a good model because this membrane has been extensively studied in the past and has a wide range of applications, including tumor growth and blood vessel analysis.[10] The experimental techniques and conditions involved in developing the CAM as an angiogenesis model have been well documented and tested.[11–15] The chicken embryo has a short gestation period and the embryo itself is easily manipulated.

The CAM is a highly vascularized, transparent, extraembryonic membrane that grows against the inner wall of the developing chicken egg. It develops between days 3 and 12 of the gestation period, and undergoes rapid angiogenesis between days 5 and 9.[16] Another type of vessel development, intussusceptive capillary growth, occurs between days 8 and 12 and is followed by a period of vessel expansion.[16] The CAM aids the developing embryo in nutrient and waste exchange with the atmosphere, especially calcium uptake from the shell and electrolyte transport from the allantoic sac.[17,18] The CAM is formed from three layers of tissue: the chorionic epithelium, the mesoderm, and the allantoic epithelium (Fig. 1).[19] The chorionic epithelium lies proximal to the shell and is derived from the chorionic ectoderm, while the mesoderm is the center tissue and consists of a highly branched vascular system that undergoes rapid angiogenesis during development. The allantoic epithelium lies distal to the shell and is derived from the allantoic ectoderm. As the CAM develops and surrounds the entire inner shell, the vasculature extends from the mesoderm into the chorionic epithelium for more efficient nutrient exchange.

The CAM model has been previously investigated using OPE-PDT.[20–23] Several groups have used the CAM to assay topically applied photosensitizing drugs *in vivo*.[20,22,23] Another more recent study (2001) performed by Lange et al.[21] tested the efficacy of several OPE-PDT photosensitizers by intravenous injection in the 12 to 13-day CAM. It was found that vasoconstriction and complete vessel closure could be induced in the CAM by irradiation with OPE light, while not affecting the structure and function of the vessels that were not irradiated. Although this paper provides a strong case for the use of the CAM as a PDT drug-screening model for AMD, intravenous TPE-PDT drug characterization can be better modeled using younger chicken embryos in which the CAM is still undergoing rapid angiogenesis (e.g., days 8 to 9). The challenge is the development of injections and monitoring protocols for TPE-PDT.

In this paper, the work performed on the CAM model has been *ex ovo* with the intention to extend it to an *in ovo* system. *Ex ovo* work has allowed the development of the techniques required to work with the CAM, while permitting the characterization of the photosensitizing drug Verteporfin within this biological system. Experimental trials on vessel ablation and the distribution and localization of liposomal Verteporfin have been performed on the 8 to 9-day-old CAM.

2 Methods and Materials

2.1 *Experimental Design*

Our TPE-PDT setup was described previously.[9] A Zeiss 20 $\times$ objective with a 1.00-cm working distance and a numerical aperture of 0.4 was used. Unless otherwise stated, the laser power ranged between 140 and 200 mW at the back aperture of the microscope, and the TPE wavelength was set at 780 nm with approximately 100-fs pulses at an 82-MHz repetition rate. Injections were made using a manual microinjector from Sutter Instruments Co. The syringe was held in place and directed by an x,y,z-micromanipulator (Sutter Instruments Co., MM-33). The needles were formed by pulling borosilicate glass capillaries (World Precision Instruments Inc.) with an outer diameter of 1.0 mm and an inner diameter of 0.58 mm, and a quick-fill inner filament. The average outer diameter of the pulled capillaries used as microneedles was 0.02 mm.

2.2 *Liposomal Verteporfin*

Dry dioleoyl-phosphatidylcholine (DOPC, Sigma Chemical Co.) was dissolved in chloroform to form a stock solution with a concentration of 10 mg/ml. Verteporfin (QLT Inc.) was dissolved in dimethyl sulfoxide (Sigma) and the concentration (1.438×10^{-4} M) was determined spectrophotometrically ($\lambda = 688$ nm, $\varepsilon = 32740$ liter$\cdot$mol$^{-1}\cdot$cm^{-1}). Liposome solutions were prepared by adding an appropriate amount of DOPC into a glass vial and evaporating all of the chloroform solvent under nitrogen. Phosphate buffer (0.02 M, pH 7.0) and stock Verteporfin were added to resuspend the dried lipid in a final solution of 0.01 mg/ml Verteporfin:1.0 mg/ml DOPC. The resultant solutions were cycled through 10 min of stirring and 10 min of sonication until the mixture cleared. We have shown that these solutions contain small unilamellar vesicles (SUVs) and small multilamellar vesicles.[24] The solutions were refrigerated in the dark for up to one week and were subjected to stirring and sonication to ensure that no large aggregates were present. Filtering the liposomal solution with a 0.02-μm hydrophilic cellulose acetate syringe filter (Albet) ensured that the solution was free of debris, such as dust, that could potentially plug the pulled capillaries.

PROOF COPY 005303JBO

PROOF COPY 005303JBO

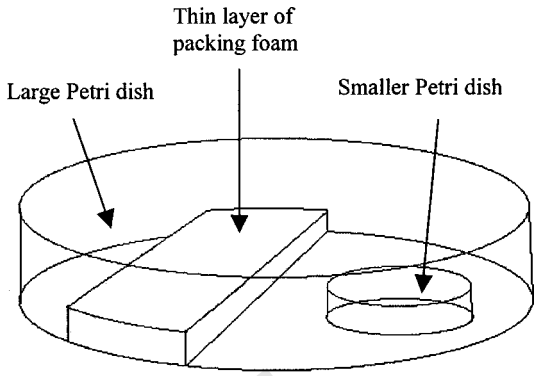

Fig. 2 Modified Petri dish for *ex ovo* CAM experimentation. The embryo is placed into a small Petri dish (4 cm diameter) that is attached to the bottom of the larger dish (10 cm diameter). The CAM is removed from the eggshell and draped across the thin layer of packing foam that is attached to the bottom of the dish. The embryo can then be covered with the lid of the Petri dish to maintain temperature and moisture until experimentation.

2.3 *Ex ovo Experiments*

Fertilized chicken eggs were obtained from the Ijtsma farm (RR 2 site 11 Box 6, Airdrie, Alberta, T4B 2A4) and stored at 14 °C until they were placed in a 38 °C, humidified incubator, without rotation, for the duration of their development. Prior to incubation and manipulation, the eggs were cleaned and sterilized with 70% ethanol. After 72 h of incubation, the eggs were removed from the incubator, and approximately 3 ml of albumin were removed from the blunt end of the egg. This permits the developing embryo to drop away from the shell and prevents the complete adhesion of the CAM membrane and tearing during *ex ovo* embryo manipulation.

Experimentation occurred on days 8 and 9 of the gestation period. The eggs were cracked into a modified Petri dish as shown in Fig. 2. The CAM was carefully removed from the eggshell with a metal spatula and laid on the sponge layer of the Petri dish. The CAM was then secured in place using small pushpins, and any excess albumin and yolk was removed with a syringe to reduce movement and to ensure proper surface tension for smooth injection. The exposed surface of the membrane was kept moist during experimentation by topically adding Howard's Ringer solution (0.1 M sodium chloride, 0.002 M calcium dichloride dihydrate, 0.005 M potassium chloride, pH 7.2) a few milliliters at a time. Injections were performed intravenously, using 1 to 2 μl of liposomal Verteporfin, depending on blood vessel size.

The depth of the laser focal spot within the CAM can be estimated by the size of the blood vessel, which is assumed to be cylindrical. Therefore, since we estimate the diameter of the blood vessels to be 15 to 50 μm, the deepest focal spot we employ is approximately 100 μm, including passing through the chorionic epithelium (up to 50 μm). The tissue above the blood vessel does not drastically alter the focal volume achieved because it is relatively transparent and will cause very little absorption and scattering of the laser light.

Two types of intravenous injection experiments were undertaken to investigate the transportation dynamics of liposomal Verteporfin in a CAM vessel. Thus two sensitizer injection protocols were followed. In the first, sensitizer was injected into a large vessel while the vessel was observed at lower magnification (5×) using reflected white light. Then the magnification was increased (20×) and the laser was focused in the center of a smaller vessel branching off the larger one (assuming the vessel is cylindrical, the center will be where the outside edges are in focus). The focal volume was therefore ''downstream'' (approximately 1 to 3 cm) from the injection site. The laser beam was then unblocked and collection of the TPE fluorescence data was initiated. This allowed more accurate injections while permitting the analysis of smaller blood vessels and capillaries closer in size to the AMD model.

In the second protocol, it was possible to position the needle so that it could be observed in the 20× objective field of view. In this instance, the needle was inserted into the blood vessel, but the injection was not performed at this time. The laser beam was unblocked and TPE fluorescence detection was initiated. Then, while the background autofluorescence count rate was being measured, the injection was performed. Thus, in the second protocol the changes in TPE-fluorescence histograms represent the entire bolus as it passes through the excitation volume. Injection sites within close proximity (2 to 3 mm) to the excitation volume allowed analysis of the transportation rates almost immediately upon entry into the blood vessel.

Prior to injection, controls were run of the background endogenous fluorescence on the surface of the CAM membrane (the chorion epithelium or the allantoic epithelium, depending on the position of the CAM) and the center of the blood vessels (representing free-flowing blood without injection). The TPE-fluorescence count rate of the liposomal Verteporfin solution examined in the open air was measured by placing a drop of solution on a glass slide. Typical results from these controls are shown in Fig. 3.

For localization studies, fluorescence readings were taken before injection at the upper surface of the CAM membrane (relative to the membrane *ex ovo*), and at the top of the vasculature tissue, the center of the vessel with free-flowing blood, and the bottom of the vasculature tissue. These readings supplied a background for endogenous fluorescence readings from the blood vessels. The liposomal Verteporfin was then injected, left for approximately 10 min to clear the vessel, and then the same four readings were taken again. Although the laser spot was not focused to exactly the same spot on the tissue for each run, the data were collected as consistently as possible by focusing the laser in the center of the blood vessel and approximating the depth of the spot within the tissue.

3 Results

3.1 *Ablation*

Ablation of blood vessel walls was successful in initiating bleeding to mimic the leaky vessels found in AMD. This effect was induced by using laser powers varying from 40 to 200 mW. Small perforations, which appeared to be analogous in shape to the laser focal volume but larger in size, could be ''cut'' into the sides of vessels, allowing blood leakage but also permitting the bulk blood to continue flowing through the vessels [Fig. 4(a)]. One can also induce complete occlusion in blood vessels, which is useful for stopping blood flow for

PROOF COPY 005303JBO

PROOF COPY 005303JBO

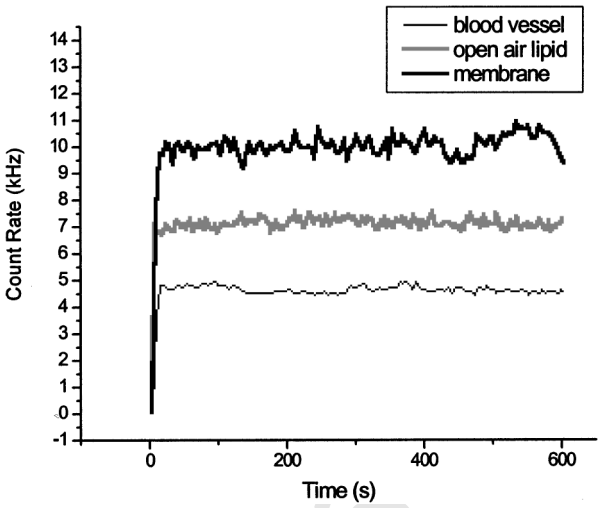

Fig. 3 Control histograms for two-photon excitation fluorescence versus time. The histogram for the blood vessel represents the endogenous fluorescence of the free-flowing blood (i.e., center of the vessel) without injection of the photosensitizer. The histogram for the surface of the membrane represents the endogenous fluorescence of the CAM without photosensitizer injection. The open-air lipid control histogram represents the resultant fluorescence from a droplet of the liposomal Verteporfin solution on a glass slide. The initial rise in the signal occurs when the shutter to the detector is opened.

analysis [Fig. 4(b)]. Often at high laser powers (120 to 200 mW), ablation was uncontrollable owing to the short period required to cause damage. As the laser power was lowered below 120 mW, the vessels perforated at a slower rate, and therefore cutting the vessels became more controllable.

3.2 *Transportation of Liposomal Verteporfin within CAM Blood Vessels*

Figure 5 is an example of two TPE-fluorescence histograms (trials 1 and 2) in which the injections were performed using the first protocol. Single exponential decays empirically described the flow of the liposomal Verteporfin through the TPE volume (~3.0 fl) and the constants for these trials are listed in Table 1 for comparison. Typical data for the trials performed using the second protocol (trials 3 and 4) are presented in Fig. 6 and the decay constants are summarized in Table 1.

We also attempted to model the data based on the one-dimensional diffusion equation:

$$I_{\mathrm{fl}}(x,t) \propto c(x,t) = \frac{c_0 \exp(-x^2/4Dt)}{2A(\pi Dt)^{1/2}}, \qquad (1)$$

where I_{fl} is the fluorescence intensity, x is an arbitrary distance away from the injection point, A is the area through which the bolus is flowing, t is time in seconds, D is the diffusion coefficient of the liposome, and c_0 is the concentration in the initial bolus. Since the transit rate (~1 mm/s) through the TPE volume is very fast compared with the diffusional spreading of the bolus, it is not unreasonable to use this model. In Fig. 6, we show an example of a modeled trailing bolus edge. The constants used were $D = 5 \times 10^{-13}$ m^2/s, $x = 1$ μm, and $A = 2$ μm^2. It was not realistic to use this equation for the data shown in Fig. 5 because fluorescence for the entire bolus was not measured in that case.

The fluorescence histograms obtained for both types of injection show a sharp initial increase and then decrease at a slower rate, creating a tailing peak that can be fitted with a single exponential decay curve. The injections made close to the excitation site have a sharper initial increase than those made at a greater distance.

3.3 *Localization of Liposomal Verteporfin within CAM Blood Vessels*

It is important to understand the localization of liposomal Verteporfin within the vasculature in order to optimize the

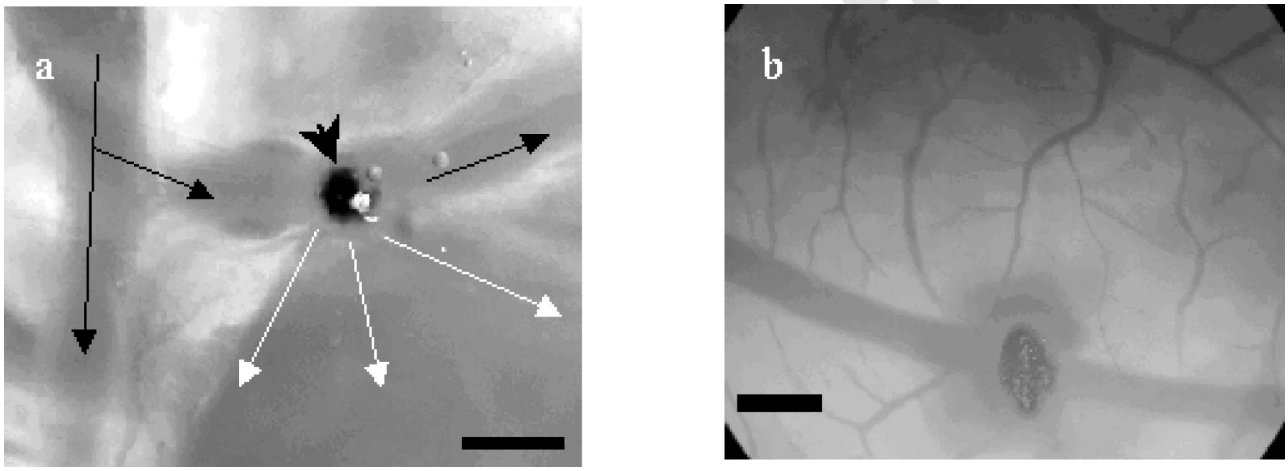

Fig. 4 Reflected light images of ablated CAM blood vessels. (a) Ablation results in the leakage of a vessel while still allowing blood to flow through the vessel. The blood vessel was ablated using several (~4) exposures to laser light of 780 nm at 190 mW for 3 s each. The black arrows show the direction of blood flow in the vessels. The arrowhead indicates the ablated spot and the white arrows indicate the leakage of blood from the vessel. (b) A blood vessel has been occluded by administration of several (~10) exposures to laser light of 780 nm at 140 mW for 3 s each. Note that there is some leakage of blood around the burn spot. Occlusion prevents blood flow in the vicinity of the cauterization. Scale bars are 100 μm.

PROOF COPY 005303JBO

PROOF COPY 005303JBO

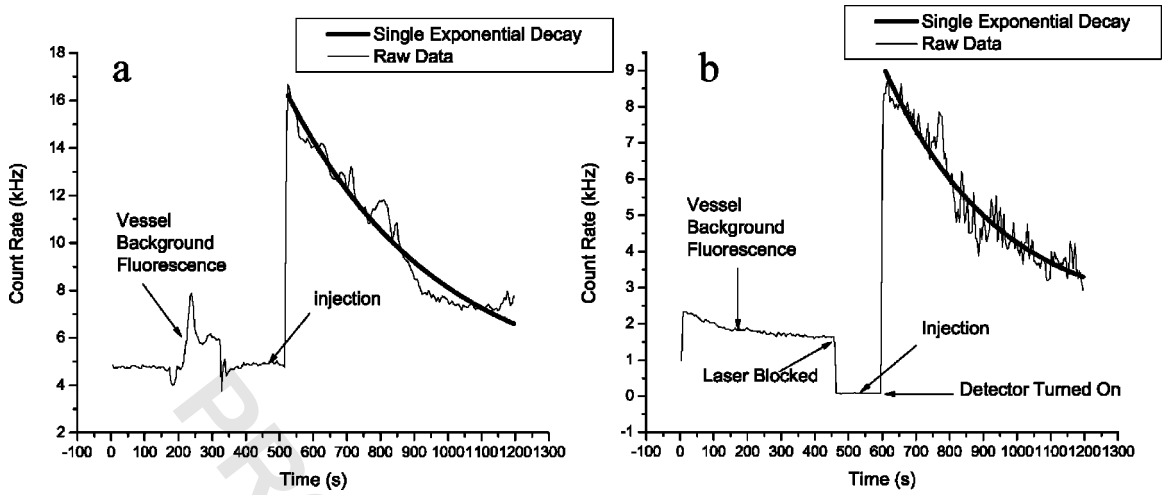

Fig. 5 Examples of two-photon excitation fluorescence resulting from liposomal Verteporfin injections during the time span of the data collection. Both decays are best fit to a single exponential decay curve with constants. (a) trial 1 and (b) trial 2. The noisy peaks in (a) prior to the injection are due to endogenous fluorescence of the blood vessel.

PDT therapy. A comparison of the fluorescence readings before and after the photosensitizer injections allows a comparison of the localization of liposomal Verteporfin within the CAM membrane. A typical example of these trials is given in Fig. 7. In this example, the overall fluorescence count rate in the membrane and in the middle and lower vasculature layers appears to increase approximately 0.75 kHz after stabilization, while the fluorescence intensity of the upper vasculature increases more significantly ($\sim$6 kHz). Therefore it can be suggested that the liposomal Verteporfin is selectively localizing on one side of the vascular network. It was possible to repeat this experiment three times, with similar results in two of the three experiments.

4 Discussion

4.1 *Ablation*

In wet AMD, new vasculature tends to be ''leaky,'' allowing fluid to escape and then to collect around the blood vessels.[2] This causes swelling of the retinal tissues and can lead to acceleration of macular dysfunction and subsequent vision loss. In developing a CAM model for the two-photon photodynamic therapy of wet AMD, leaky blood vessels must be created. This was accomplished by ablating normally healthy vascular tissue in the CAM and causing the photosensitizer to collect around the blood vessel. Thus the porous conditions found in AMD can be mimicked and studied. We found that lesions approximately 30 μm in diameter could be opened in vessel walls using a focused laser beam operating between 40 and 120 mW. The diameter of the perforation is larger than the focused TPE beam waist ($\sim$2 μm), most likely because of shock waves coupling to the surrounding vessel tissue during ablation.

Complete occlusion of the blood vessels allows *in vitro* controls to be used on the biological tissue. By stopping blood flow completely, the fluorescence of the liposomal bolus can be measured without the added variable caused by directional flow of the blood. In the future, occlusion will allow us to observe the conditions under which photobleaching can occur.

Table 1 Summary of first exponential rate constants for the distribution experiments.

Trial Number	Time of Injection	Decay Constant (s)
1	During	2.2×10^{-3}
2	During	3.0×10^{-3}
3	Prior	1.2×10^{-3}
4	Prior	3.1×10^{-3}

4.2 *Transportation of Liposomal Verteporfin within CAM Blood Vessels*

Initially the transportation rates of liposomal Verteporfin were investigated to determine the photobleaching rates *in vitro*. Based on the open air and stopped blood flow controls of liposomal Verteporfin (not shown), it was established that photobleaching was not occurring, which allowed the dynamics of drug distribution to be examined. Under similar low laser-intensity conditions, we have shown that the TPE photobleaching rate is minimal.[29]

The shape of the fluorescence histogram as the bolus of liposomal Verteporfin in CAM blood vessels passes through the excitation volume is best modeled by a single exponential decay. We have also attempted to model the transit of the bolus using 1-D diffusion, which may be appropriate in a blood vessel (see Fig. 6). The 1-D diffusion represents the spreading out of the trailing end of the bolus by diffusion while the leading edge remains compacted by the flow. Thus, the bolus has 300 to 500 s to diffusively spread from its initial distribution while flowing from the point of injection to the location in the vessel where the laser beam is focused. The lack of total agreement between the 1-D diffusional model and the data most likely indicate that there is a component of diffusion perpendicular to the flow axis. Moreover, since we

PROOF COPY 005303JBO

PROOF COPY 005303JBO

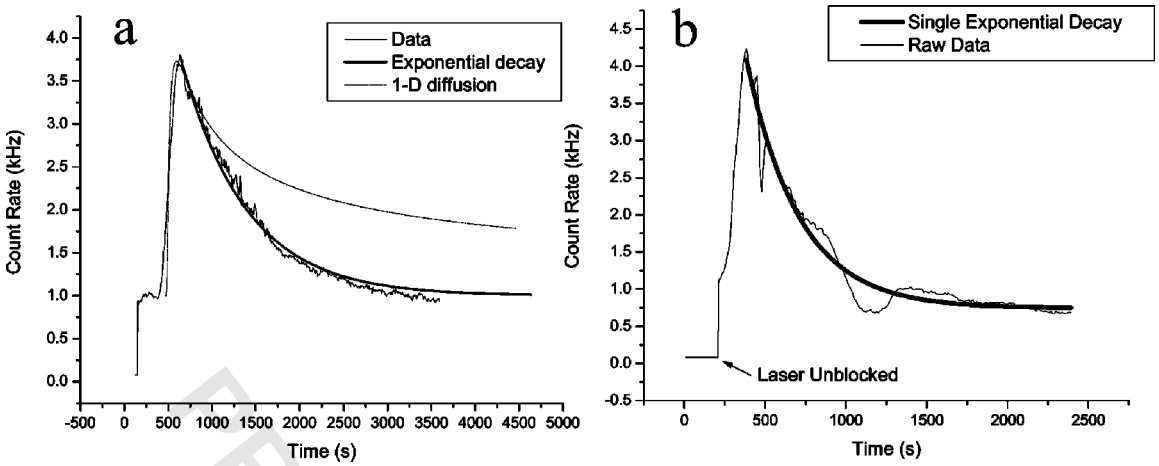

Fig. 6 Examples of two-photon excitation fluorescence resulting from liposomal Verteporfin injections prior to the start of fluorescence detection. These yield decay curves that best fit single exponential decays. These curves are typical examples of the fluorescence data collected. (a) Trial 3, which includes an example of a 1-D diffusional model for the bolus spreading, and (b) trial 4.

observe no evidence of photobleaching, the difference in the 1-D diffusion model and the data cannot be explained by the reaction of the sensitizer.

As can be observed from comparing the histograms of Fig. 5 and Fig. 6, the closer the drug bolus is injected to the excitation volume, the sharper the initial fluorescence increase. The injections that were made at a greater distance from the excitation volume do not have as sharp an initial increase and have a longer tail, again suggestive of diffusional spreading. The variation in fluorescence intensity before to the point of injection in these histograms is due to the endogenous fluorescence of the blood vessels and possible slight movement of the CAM.

A peak with this same shaped has been observed in other blood flow studies involving the intravenous injection of a fluorescent drug bolus. In 2002, Ossewaarde-Van Norel et al.[25] undertook a study to quantify retinal dye leakage during routine ocular fluorescein angiographies. Although these experiments were performed with a different intent, the injection of a bolus of fluorescent drug provided histograms similar to those shown here. There are several important differences between the histograms observed in the retina and the CAM. First, the initial intensity peak is much sharper in the retinal study, which indicates a tighter bolus of drug. This was the intent of the authors in order to quantify the concentration, but is not required in our work. Another difference is that the retinal histograms are integrated over a larger collection area and may include up to 10% background fluorescence from other retinal blood vessels and areas adjacent to the vessel in question. The CAM TPE-fluorescence is confined to a single blood vessel so that background fluorescence from the surrounding tissue is eliminated.

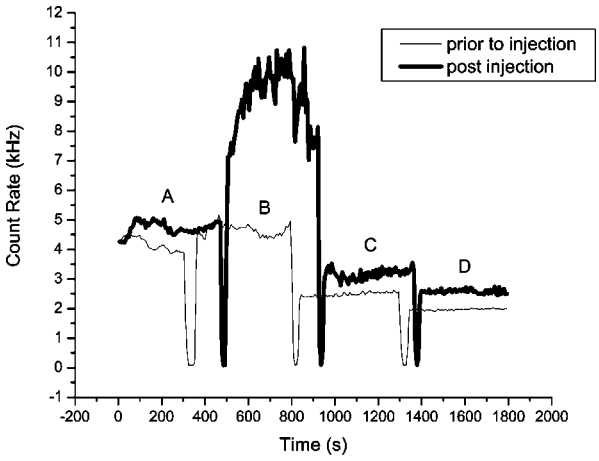

Fig. 7 A typical result determined by observing the different layers of the CAM membrane and vessels within the membrane. Each two-photon excitation fluorescence plot has four distinct sections: (a) the surface of the membrane; (b) the top of the vessel wall (relative to the membrane *ex ovo*); (c) the center of the vessel, including free-flowing blood; and (d) the bottom of the vessel wall. The liposomal Verteporfin appears to localize along the upper wall of the vasculature when considering the fluorescence increase in (b) after injection.

4.3 *Localization of Liposomal Verteporfin in CAM Blood Vessels*

From Fig. 7 it can be seen that the fluorescence intensity of the controls decreases as the depth of the reading into the tissue increases. This is intuitive because light scatter and reabsorption of the fluorescence by the tissue increases as the laser beam travels further through the tissue.

First, we have to consider whether we can realistically focus the laser beam within each of these tissue layers. The thickness of the vessel wall (ΔD) has been estimated in previous work to be $\Delta D \approx 0.1D$, where D is the diameter of the blood vessel in question.[26] For the vessels in the present study, we estimate diameters of 15 to 50 μm and thus vessel wall thicknesses of 1.5 to 5.0 μm. The TPE depth of focus is 4 μm, which means that the excitation volume can be confined to regions containing the vessel walls and to free-flowing blood.

After the sensitizer bolus had cleared the excitation volume, the overall increase in fluorescence intensity throughout the three layers suggests that liposomal Verteporfin is localizing in trace amounts throughout the tissue. The largest fluorescence increase is observed on the upper vessel wall, which

PROOF COPY 005303JBO

PROOF COPY 005303JBO

suggests that there is some mode of localization for liposomal Verteporfin. The chorionic epithelium that lies proximal to the eggshell contains villus projections with an intraepithelial vasculature originating from the mesoderm.[19] These villi are believed to function in transport of calcium, other nutrients, and waste products between the shell membrane and the circulatory system. Active pinocytosis has also been observed from these cells, and vesicles are often found in the surrounding areas, indicating a vesicle-mediated delivery system.[18,27,28] This suggests that there is a constant rearrangement of the lipid bilayers within these cells and the surrounding vasculature, and therefore liposomal Verteporfin may easily localize in this tissue layer.

Although the liposomal photosensitizer may not localize in the human vasculature system in the same manner as in the CAM membrane, there will be localization of the photosensitizer in the newly formed blood vessels in the eye. In AMD, the blood vessels grow outward from the choriocapillaris toward the retinal tissue;[3] therefore one would expect that localization of the photosensitizer would be greatest on the vascular tissue proximal to the photoreceptors and the RPE, compared with the vascular tissue distal from these tissue layers.

Optical factors such as fluorescence reabsorption and light scattering can be ruled out as the primary causative factor for the large increase in only one tissue layer. Preliminary absorption and emission experiments using Verteporfin show that reabsorption is minimal in solutions with concentrations comparable to those used here (10^{-6} M or less).[29] Therefore, if Verteporfin is being evenly distributed throughout the vascular tissue and the blood, one would expect this to be reflected in the histograms by a similar increase in fluorescence intensity throughout each tissue layer. However, we observed a fivefold increase in the sensitizer fluorescence in the upper vessel wall compared with the other environments.

Determining the area of localization will allow more specific treatment conditions. By limiting the excitation volume to the tissue layer with the greatest amount of photosensitizer, the PDT treatment can be optimized and the probability of vessel closure can be increased.

Ex ovo CAM experimentation is limited by several important factors. First, the embryo will eventually cool down and dry out if data analysis is performed for a long period of time. When fluorescence data are being collected, Ringer's solution cannot be added to the system to maintain moisture without changing the depth of focus. This prevents the observation of the membrane over several days to ensure TPE-PDT-induced vessel closure. Second, removing the CAM from the eggshell often damages the membrane itself. This can be avoided by incubating the eggs from day 3 *in vitro*, but it has been shown that the embryo's development will be slower and will often have growth defects.[12,15] The vascularization of the CAM does appear to be similar to that of an embryo incubated *in ovo*.[11] These limitations can be overcome by incubating and experimenting with the CAM *in ovo*, which is more challenging experimentally, but is our future direction in this work.

Acknowledgments

This research is supported by the Natural Sciences and Engineering Council of Canada and the Canadian Institute for Photonics Innovation. KSS is grateful for support from eMPOWR and the Alberta Ingenuity Fund in the form of scholarships. The support of QLT Inc. is enthusiastically acknowledged. The authors thank Professor Doug Muench (University of Calgary) for the use of his capillary puller and Professor Cairine Logan for many helpful discussions on chicken embryology.

References

1. M. R. Van Newkirk, M. B. Nanjan, J. J. Wang, P. Mitchell, H. R. Taylor, and C. A. McCarty, ''The prevalence of age-related maculopathy—The Visual Impairment Project,'' *Ophthalmology* **107**(8), 1593–1600 (2000).
2. S. T. Leu, S. Batni, M. J. Radeke, L. V. Johnson, D. H. Anderson, and D. O. Clegg, ''Drusen are cold spots for proteolysis: expression of matrix metalloproteinases and their tissue inhibitor proteins in age-related macular degeneration,'' *Exp. Eye Res.* **74**(1), 141–154 (2002).
3. P. A. Campochiaro, P. Soloway, S. J. Ryan, and J. W. Miller, ''The pathogenesis of choroidal neovascularization in patients with age-related macular degeneration,'' *Molec. Vision* **5**, 34–38 (1999).
4. E. M. Stone, V. C. Sheffield, and G. S. Hageman, ''Molecular genetics of age-related macular degeneration,'' *Human Molec. Genet.* **10**(20), 2285–2292 (2001).
5. P. K. Frederiksen, M. Jorgensen, and P. R. Ogilby, ''Two-photon photosensitized production of singlet oxygen,'' *J. Am. Chem. Soc.* **123**(6), 1215–1221 (2001).
6. W. G. Fisher, W. P. Partridge, C. Dees, and E. A. Wachter, ''Simultaneous two-photon activation of type-I photodynamic therapy agents,'' *Photochem. Photobiol.* **66**(2), 141–155 (1997).
7. J. D. Bhawalkar, N. D. Kumar, C. F. Zhao, and P. N. Prasad, ''Two-photon photodynamic therapy,'' *J. Clin. Laser Med. Surg.* **15**(5), 201–204 (1997).
8. R. L. Goyan and D. T. Cramb, ''Near-infrared two-photon excitation of protoporphyrin IX: photodynamics and photoproduct generation,'' *Photochem. Photobiol.* **72**(6), 821–827 (2000).
9. R. Goyan, R. Paul, and D. T. Cramb, ''Photodynamics of latex nanospheres examined using two-photon fluorescence correlation spectroscopy,'' *J. Phys. Chem.* **105**(12), 2322–2330 (2001).
10. D. Ribatti, B. Nico, A. Vacca, L. Roncali, P. H. Burri, and V. Djonov, ''Chorioallantoic membrane capillary bed: a useful target for studying angiogenesis and anti-angiogenesis in vivo,'' *Anat. Rec.* **264**(4), 317–324 (2001).
11. B. E. Dunn and T. P. Fitzharris, ''Differentiation of the chorionic epithelium of chick embryos maintained in shell-less culture,'' *Dev. Biol.* **71**, 216–227 (1979).
12. B. E. Dunn, ''Technique for shell-less culture of the 72-hour avian embryo,'' *Poultry Sci.* **53**, 409–412 (1974).
13. L. M. Kirchner, S. P. Schmidt, and B. S. Gruber, ''Quantitation of angiogenesis in the chick chorioallantoic membrane model using fractal analysis,'' *Microvasc. Res.* **51**(1), 2–14 (1996).
14. M. Nguyen, Y. Shing, and J. Folkman, ''Quantitation of angiogenesis and antiangiogenesis in the chick choriallantoic membrane,'' *Microvasc. Res.* **47**, 31–40 (1994).
15. B. E. Dunn and M. A. Boone, ''Growth of the chick embryo *in vitro*,'' *Poultry Sci.* **55**, 1067–1071 (1976).
16. P. Schlatter, M. F. Konig, L. M. Karlsson, and P. H. Burri, ''Quantitative study of intussusceptive capillary growth in the chorioallantoic membrane (CAM) of the chicken embryo,'' *Microvasc. Res.* **54**(1), 65–73 (1997).
17. M. E. Stewart and A. R. Terepka, ''Transport functions of the chick chorio-allanoic membrane. I. Normal histology and evidence for active electrolyte transport from the allantoic fluid, *in vivo*,'' *Exp. Cell Res.* **58**, 93–106 (1969).
18. A. R. Terepka, M. E. Stewart, and N. Merkel, ''Transport functions of the chick chorio-allantoic membrane. II. Active calcium transport, *in vivo*,'' *Exp. Cell Res.* **58**, 107–117 (1969).
19. W. S. Lusimbo, F. A. Leighton, and G. A. Wobeser, ''Histology and ultrastructure of the chorioallantoic membrane of the mallard duck (*Anas platyrhynchos*),'' *Anat. Rec.* **259**(1), 25–34 (2000).
20. V. Gottfired, R. Davidi, C. Acerbuj, and S. Kimel, ''*In vivo* damage to chorioallantoid membrane blood vessels by porphycene-induced photodynamic therapy,'' *J. Photochem. Photobiol. B* **30**, 115–121 (1995).

PROOF COPY 005303JBO

PROOF COPY 005303JBO

21. N. Lange, J.-P. Ballini, G. Wagnieres, and H. van den Bergh, ''A new drug-screening procedure for photosensitizing agents used in photodynamic therapy for CNV,'' *Invest. Ophthalmol. Visual Sci.* **42**(1), 38–46 (2001).
22. M. J. Hammer-Wilson, L. Akian, J. Espinoza, S. Kimel, and M. W. Berns, ''Photodynamic parameters in the chick chorioallantoic membrane (CAM) bioassay for topically applied photosensitizers,'' *J. Photochem. Photobiol., B* **53**(1–3), 44–52 (1999).
23. R. Hornung, M. J. Hammer-Wilson, S. Kimel, L. H. Liaw, Y. Tadir, and M. W. Berns, ''Systemic application of photosensitizers in the chick chorioallantoic membrane (CAM) model: photodynamic response of CAM vessels and 5-aminolevulinic acid uptake kinetics by transplantable tumors,'' *J. Photochem. Photobiol., B* **49**(1), 41–49 (1999).
24. Z. V. Leonenko, A. Carnini, and D. T. Cramb, ''Supported planar bilayer formation by vesicle fusion: the interaction of phosolipid vesicles with surfaces and the effect of gramicidin on bilayer properties using atomic force microscopy,'' *Biochim. Biophys. Acta* **1509**, 131–147 (2000).
25. J. Ossewaarde-Van Norel, P. R. van den Biesen, J. van de Kraats, and T. T. J. M. Berendschot, ''Comparison of fluorescence of sodium fluorescein in retinal angiography with measurements *in vitro*,'' *J. Biomed. Opt.* **7**(2), 190–198 (2002).
26. K. Sandau and H. Kurz, ''Modelling of vascular growth processes: A stochastic biophysical approach to embryonic angiogenesis,'' *J. Microsc.* **175**(3), 205–213 (1994).
27. R. Narbaitz, ''Structure of the intra-chorionic blood sinus in the chick embryo,'' *J. Anat.* **124**(2), 347–354 (1977).
28. R. Akins and R. S. Tuan, ''Transepithelial calcium transport in the chick chorioallantoic membrane. II. Compartmentalization of calcium during uptake,'' *J. Cell Sci.* **105**(2), 381–388 (1993).
29. R. Goyan, ''Investigations into two-photon photodynamic therapy,'' PhD Dissertation, Univ. of Calgary (2002).

PROOF COPY 005303JBO

PROOF COPY 005303JBO